FEATURE ARTICLE

Development of Accurate Quantum Dynamical Methods for Tetraatomic Reactions

John Z. H. Zhang,* Jiqiong Dai, and Wei Zhu

Department of Chemistry, New York University, New York, New York 10003

Received: July 11, 1996; In Final Form: December 5, 1996[⊗]

The time-dependent quantum wavepacket approach has proven to be a powerful computational approach for studying large scale quantum reactive scattering problems involving three or more atoms. This article presents an account of some recent development of time-dependent wavepacket methods for accurate quantum dynamics calculation of tetraatomic reactions in full dimensional space. The salient features of the time-dependent approach and important computational strategies that have been employed to successfully calculate state-specific reaction dynamics for realistic four-atom reactions are discussed. Some results from the application of the time-dependent methods to several specific reactions, in particular the benchmark $H_2 + OH$ reaction, are presented. The article is then highlighted with the presentation of a general reactant−product decoupling method for state-to-state reactive scattering study. Finally, the future outlook of the theoretical study of polyatomic reaction dynamics is discussed.

I. Introduction

The ability to accurately predict the outcome of a chemical reaction in detail on the basis of first principles has long been a holy grail for theoretical chemists since the discovery of quantum mechanics in 1920s. It was known that chemical reactions are results of molecular collision processes which can be rigorously described by quantum reactive scattering theory. In principle, the whole scenario seems rather straightforward. First, one performs *ab initio* quantum chemistry calculations to generate electronic energies at various nuclear configurations and to fit them into a global potential energy surface. Second, one performs quantum reactive scattering calculations to obtain detailed dynamics informations such as reaction probabilities, cross sections, rate constants, *etc*. In practice, however, such theoretical endeavors are a formidable computational task at best because quantitatively accurate calculations for the majority of chemical reactions are enormously complex due to inherent mathematical difficulties in solving the many-body Schrödinger equation.

Beside huge computational costs required in electronic structure calculations to generate accurate potential energy surfaces, which is outside the topic of the present article, the quantum reactive scattering calculation itself presents a major challenge to theoretical dynamicists in the study of reaction dynamics. From the very beginning, the theory of quantum reactive scattering has focused on the development of computational methodologies for atom−diatom reaction $A + BC$: the simplest possible chemical reaction systems. In particular, the $H + H_2$ and its isotopically substituted reactions have dominated the theoretical and computational study in reactive scattering for more than two decades.[1,2] Since the first report of three-dimensional quantum calculations for the $H + H_2$ reaction on the empirical PK2 potential energy surface in 1976,[1] it took another decade or so for theoretical chemists to fully develop general and powerful numerical methods to compute atom−diatom reactions. Thanks to the development of new computational methods[3−11] and the rapid increase in the speed of modern computers, tremendous progress has been made during the past decade in the theory and computation of atom−diatom reactive scattering. Rigorous and detailed quantum dynamics calculations for $H + H_2$ and other simple triatomic reactions in three-dimensional space have been reported, and some excellent agreements between exact quantum dynamics calculations and experiments have been obtained for $H + H_2$ and its isotopic reaction using algebraic variational methods and hyperspherical coordinate methods as recently reviewed in ref 2. Very recent dynamics calculations for $H + H_2$[12] and $F + H_2$[13] show that the remaining discrepancy between dynamics calculation and experiment for these two systems appears to be entirely attributable to the deficiency in the part of the potential energy surface (PES) or its proper treatment in the dynamics calculation, not in the part of the dynamics calculation itself.

Of more practical interest to chemistry communities is, however, polyatomic reactions that involve more than three atoms. But going beyond the atom−diatom to polyatomic reactive scattering presents a new grand challenge to quantum dynamicists. The major challenge in theoretical treatment is how to handle the exponential increase of computational cost due to the increase of mathematical dimensionalities when the number of atoms in the system increases. For example, the dimensionality (internal degrees of freedom) increases from three for a triatomic system to six for a tetraatomic system—a two-fold increase in dimensionality! Since the addition of each atom adds three internal degrees of freedom to the system, it is interesting to note that the transition from triatomic to tetra-atomic systems causes the maximum relative increase in dimensionality (100%). Thus the rigorous dynamical treatment for tetraatomic reactions is hardly a trivial extension of the previous treatments for triatomic reactions and its success is a major advance in reaction dynamics. In fact, a number of computational methodologies that work effectively for simple triatomic systems prove difficult or even impossible to apply at present to polyatomic reactions due to the requirement of impractically large computational resources. For example, in

[⊗] Abstract published in *Advance ACS Abstracts,* March 15, 1997.

S1089-5639(96)02073-7 CCC: $14.00

algebraic variational approach, one is required to invert the Hamiltonian matrix to solve linear algebraic equations. Even for a simple tetraatomic reaction like $H_2 + OH$, the size of the Hamiltonian matrix is prohibitively too large to be inverted directly on today's computers. It is therefore necessary to utilize alternative methods such as iterative methods to solve linear algebraic equations due to their lower computational scaling than that of matrix inversion. Thus the critical measure of the applicability of any method to polyatomic reactions is the scaling of its computational cost with respect to the number of basis functions or degrees of freedom. Many standard time-independent scattering methods such as variational methods or propagation methods scale as N^3 with the number of basis functions N and are thus difficult to extend to large systems. Until a few years ago, the reduced dimensionality approach (RDA) of Bowman and co-workers[14] and Clary and co-workers[15] provided the only viable means for tackling the four-atom reactive scattering problem in which a four-atom reaction system is reduced to an effective atom−diatom system through elimination of three internal coordinates, either by applying adiabatic approximation for three internal angular variables[14] or by restricting the system to certain geometric configurations.[15] Although the RDA methods are computationally simple to apply and can often give reasonably good results when all the missing degrees of freedom are properly accounted for, they generally do not give definitive results and/or predictions of the dynamics of the reactive scattering problem for a given potential energy surface. The status is similar for other dynamically approximate methods including the IOSA method,[16] the mixed quantum/classical method,[17] and full-dimensional planar models.[18−20] These approximate methods are very useful for studying the dynamics of complex reactions for which rigorous dynamical methods are not available.

The ultimate goal in quantum reaction dynamics is to develop rigorous quantum methods that can provide definitive results and/or predictions for dynamics of polyatomic reactions for given potential energy surfaces. Significant progress has been made in that direction during the past few years, and the above goal has been at least partially realized for a few important benchmark tetraatomic reactions. Rigorous quantum reactive scattering calculations in full-dimensional space have been reported for reactions of $H_2 + OH$,[21−25] $DH + OH$,[26,27] $D_2 + OH$,[28] and $HO + CO$,[29] including calculations of initial state specific cross sections for $H_2 + OH$ and its isotope reactions.[22,23,27,28] Most recently, quantum state-to-state calculations have become available for the $H_2 + OH$ reaction[30,31] and its reverse reaction $H + H_2O$.[32,33]

The main driving force behind the recent success of rigorous quantum dynamics studies for tetraatomic reactions mentioned above is the development of efficient time-dependent (TD) methods for solving the time-dependent Schrödinger equation[34]

$$i\hbar\frac{\partial}{\partial t}\Psi(t) = H\Psi(t) \tag{1.1}$$

The TD wavepacket approach has some very attractive features for large-scale numerical calculations. The most fundamental property of the TD approach is that it solves an initial value problem and calculates the wave function for one initial state at a time. Therefore, for any desired initial state, the computational effort in the TD approach is proportional to N^α ($1 < \alpha < 2$)[35,36] where N is the number of basis functions (a very large number). This reduction in computational scaling is crucial for large-scale quantum calculations as mentioned above. Also in the TD approach, a single wavepacket calculation can give dynamical quantities such as **S** matrix elements or reaction probabilities over a wide range of energies. The TD approach of directly provides dynamics information in real time which greatly facilities the analysis of the underlying dynamics. We will present in this article some basic computational methods and numerical techniques of the TD wave packet approach to reactive scattering problems as well as some applications of the methods to realistic four-atom reactions in order to help provide a clear picture of the status of recent theoretical/computational development in this field. Most computational results presented in this article are for the benchmark $H_2 + OH$ reaction. In addition, we will also present a newly developed general reactant−product decoupling (RPD) method which is extremely promising for future state-to-state reactive scattering studies of polyatomic reactions.

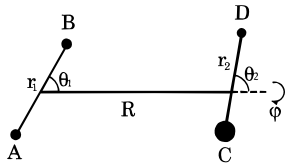

Figure 1. Jacobi coordinates for the reaction $AB + CD \rightarrow A + BCD$. The angle ϕ is the out-of-plane torsional angle.

This article is organized as follows: Section II presents the general methodology of the time-dependent wavepacket approach to quantum reactive scattering and various numerical techniques that are crucial to the success of the TD approach to large scale reactive scattering calculations for polyatomic reactions. Section III presents some benchmark results from the applications of the TD methods to several important tetraatomic reactions including $H_2 + OH$ and its isotopically substituted reactions and the resonance-dominated $HO + CO$ reaction. In section IV, we discuss a new and general methodology for efficient calculation of state-to-state reactive scattering dynamics for polyatomic reactions using the idea of divide and conquer. Finally, we give a brief discussion about the future prospect of the TD approach and speculate on possible future directions in this field.

II. Time-Dependent Wavepacket Approach

A. Selection of Coordinates and Basis Functions. In this section, we are primarily interested in the calculation of total (final state summed) reaction probabilities while the discussion on complete state-to-state reactive scattering calculation will be given in the following sections. As is well-known to the reactive scattering community, the choice of suitable coordinates, as well as the basis functions associated with them is at the heart of any reactive scattering problem. The Jacobi coordinates are natural coordinates for describing wave functions that are confined primarily to the corresponding arrangement channel space. Thus, the Jacobi coordinates of the reactant arrangement is generally a good choice for calculating initial-state-selected but final-state-summed reaction probabilities because we only need to propagate the wave function to just beyond the transition state region. Specifically for a diatom−diatom reaction $AB + CD$ to produce atom−triatom products $A + BCD$ and/or $B + ACD$, the Hamiltonian expressed in the reactant Jacobi coordinates shown in Figure 1 in full dimensions (6D) can be written as

$$H = -\frac{\hbar^2}{2\mu}\frac{\partial^2}{\partial R^2} + \frac{(\vec{J} - \vec{j}_{12})^2}{2\mu R^2} + h_1(r_1) + h_2(r_2) + \frac{\vec{j}_1^{\,2}}{2\mu_1 r_1^2} + \frac{\vec{j}_2^{\,2}}{2\mu_2 r_2^2} + V(\vec{r}_1, \vec{r}_2, \vec{R}) \tag{2.1}$$

where μ is the reduced mass between the center-of-mass of AB and CD, $\vec{J}$ the total angular momentum operator, and $\vec{j}_1$ and $\vec{j}_2$ the rotational angular momentum operators of AB and CD, which are coupled to form $\vec{j}_{12}$. The reference diatomic vibrational Hamiltonian $h_i(r_i)$ ($i = 1$ and 2) is defined as

$$h_i(r_i) = -\frac{\hbar^2}{2\mu_i}\frac{\partial^2}{\partial r_i^2} + V_i(r_i) \tag{2.2}$$

whose eigenfunctions and eigenenergies are ϕ_{v_i} and ϵ_{v_i}, respectively, and V_i is a reference diatomic vibrational potential. The expression for the Hamiltonian given in terms of the Jacobi coordinates for the A + BCD arrangement is very similar.

Before the numerical solution for the TD wave function can be started, one needs to find a suitable basis set to expand the TD wave function. For a general diatom−diatom reaction of the type AB + CD, one can expand the TD wave function in terms of body-fixed (BF) rovibrational eigenfunctions defined in terms of the reagent Jacobi coordinates as[22,23]

$$\Psi^{JM\epsilon}_{v_0 j_0 K_0}(\vec{R}, \vec{r}_1, \vec{r}_2, t) = \sum_{n,v,j,K} F^{JM\epsilon}_{nvjK,v_0 j_0 K_0}(t) u_n^{v_1}(R)\phi_{v_1}(r_1)\phi_{v_2}(r_2) Y^{JM\epsilon}_{jK}(\hat{R}, \hat{r}_1, \hat{r}_2) \tag{2.3}$$

where n is the translational basis label, v denotes (v_1, v_2), j denotes (j_1, j_2, j_{12}), (v_0, j_0) the initial rovibrational state, and ϵ the parity of the system defined as $\epsilon = (-1)^{j_1+j_2+L}$ with L being the orbital angular momentum quantum number. The determination of the TD coefficient $F^{JM\epsilon}_{nvjK,v_0 j_0 K_0}(t)$ gives the solution of the TD Schrödinger equation. In order to save computational costs, we separate the interaction region from the asymptotic region in the dynamics calculation.[37−39] A simple way to implement this is to use nondirect product basis functions, similar to the ideas of ref 37−39 and to define normalized translational basis function as

$$u_n^{v_1}(R) = \begin{cases} \sqrt{\dfrac{2}{R_4 - R_1}} \sin\dfrac{n\pi(R - R_1)}{R_4 - R_1} & v_1 \le v_{\text{asy}} \\ \sqrt{\dfrac{2}{R_2 - R_1}} \sin\dfrac{n\pi(R - R_1)}{R_2 - R_1} & v_1 > v_{\text{asy}} \end{cases} \tag{2.4}$$

where R_2 and R_4 define, respectively, the interaction and asymptotic grid,[23] and v_{asy} is the number of energetically open vibrational states plus a few closed vibrational states of the reactive AB diatom. The use of nondirect product basis makes it simple to separate the asymptotic region from the interaction region, and thus a substantial amount of computational savings can be realized.[21−23]

The coupled total angular momentum eigenfunctions $Y^{JM\epsilon}_{jK}$ in eq 2.3 can be written as[23,40,41]

$$Y^{JM\epsilon}_{jK} = (1 + \delta_{K0})^{-1/2}\sqrt{\frac{2J+1}{8\pi}}\,[D^J_{K,M} Y^{j_{12}K}_{j_1 j_2} + \epsilon(-1)^{j_+ + j_2 + j_{12} + J} D^J_{-K,M} Y^{j_{12}-K}_{j_1 j_2}] \tag{2.5}$$

where $D^J_{K,M}(\Theta\Phi\Psi)$ is the Wigner rotation matrix[42] with three Euler angles($\Theta\Phi\Psi$) and $Y^{j_{12}K}_{j_1 j_2}$ is the angular momentum eigenfunction of j_{12},[23,40,41]

$$Y^{j_{12}K}_{j_1 j_2}(\theta_1, \theta_2, \phi) = \sum_{m_1}\langle j_1 m_1 j_2 K - m_1 | j_{12} K\rangle y_{j_1 m_1}(\theta_1, 0) y_{j_2 K - m_1}(\theta_2, \phi) \tag{2.6}$$

where y_{jm} are spherical harmonics. Note in eq (2.5) the restriction $\epsilon(-1)^{j_1+j_2+j_{12}+J} = 1$ for $K = 0$.

B. Time Propagation of the Wave Function. The split-operator propagator[43] is used to carry out the time propagation of the wavepacket

$$\Psi^{JM\epsilon}(\vec{R}, \vec{r}_1, \vec{r}_2, t+\Delta) = e^{-iH_0\Delta/2} e^{-iU\Delta} e^{-iH_0\Delta/2} \Psi^{JM\epsilon}(\vec{R}, \vec{r}_1, \vec{r}_2, t) \tag{2.7}$$

where the reference Hamiltonian H_0 is defined as

$$H_0 = -\frac{\hbar^2}{2\mu}\frac{\partial^2}{\partial R^2} + h_1(r_1) + h_2(r_2) \tag{2.8}$$

and the effective potential of operator U in eq 2.7 is defined as

$$U = \frac{(\vec{J} - \vec{j}_{12})^2}{2\mu R^2} + \frac{\vec{j}_1^{\,2}}{2\mu_1 r_1^2} + \frac{\vec{j}_1^{\,2}}{2\mu_2 r_2^2} + V(\vec{r}_1, \vec{r}_2, \vec{R}) = V_{\text{rot}} + V(\vec{r}_1, \vec{r}_2, \vec{R}) \tag{2.9}$$

The matrix version of eq 2.7 for the expansion coefficient vector **F** is then given by

$$\mathbf{F}(t + \Delta) = \exp(-i\mathbf{H_0}\Delta/2)\exp(-i\mathbf{U}\Delta)\exp(-i\mathbf{H_0}\Delta/2)\mathbf{F}(t) \tag{2.10}$$

where $\mathbf{H}_0$ is the diagonal matrix defined in ref 23.

At a given quadrature point (R_m, r_{1n}, r_{2l}), the standard method for handling the potential operator $e^{-iU\Delta}$ is by diagonalizing the potential matrix **U** in the coupled angular basis $Y^{JM\epsilon}_{jK}$ as is done in previous studies.[21−23] This approach preserves the unitarity of the operator $e^{-iV\Delta}$ and is efficient when the size of the angular basis $Y^{JM\epsilon}_{jK}$ is relatively small. However, if the coupled angular basis is large, this approach can become computationally expensive because one needs to calculate and store all the transformation matrices that diagonalize the potential matrices **U** at all the radial grid points. Thus for large systems, the matrix diagonalization method will require a large-memory computer. We thus devise a normalized quadrature scheme for treating angular quadratures which avoids explicit matrix diagonalization and therefore does not require large computer memory for matrix storage. It is worthwhile to point out that this normalization procedure is only necessary when multidimensional nondirect product basis functions, such as the coupled angular momentum eigenfunctions of eq 2.6, are used. For direct product basis functions, one can use the DVR method to rigorously preserve the unitarity of the propagator. This normalization procedure has been discussed in ref 27 and 28 and we present it briefly in the following.

Utilizing the split-operator scheme again, we can split $e^{-iU\Delta}$ as

$$e^{-iU\Delta} = e^{-iV_{\text{rot}}\Delta/2}\, e^{-iV\Delta}\, e^{-iV_{\text{rot}}\Delta/2} \tag{2.11}$$

where V_{rot} and V are defined in eq 2.9. The operation of the operator $e^{-iV_{\text{rot}}\Delta/2}$ on the wave function is straightforward because it is diagonal in the coupled angular momentum representation. The exponential potential operator $e^{-iV\Delta}$ is now treated by quadrature approximation for which we define a transformation matrix **Q** by

$$Q^{iK}_{ikl} = \sqrt{W_{1i}W_{2k}W_l}\,\langle\theta_{1i}\theta_{2k}\,\phi_l | Y^{JM\epsilon}_{jK}\rangle \tag{2.12}$$

where (θ_{1i} θ_{2k} ϕ_l) are angular quadratures and ($W_{1i}W_{2k}W_l$) are the corresponding angular weights. Thus eq 2.11 is ap-

proximated by the angular quadrature

$$e^{-iU\Delta} = e^{-iV_{\rm rot}\Delta/2}\,\mathbf{Q}^{+}\,e^{-iV\Delta}\,\mathbf{Q}e^{-iV_{\rm rot}\Delta/2} \qquad (2.13)$$

where $\mathbf{Q}^{+}$ is the complex conjugate of $\mathbf{Q}$. In general, one does not need to store the large matrix $\mathbf{Q}$ but only a few small submatrices contained in eq 2.12.

Because the transformation matrix $\mathbf{Q}$, which transforms from coupled angular momentum representation to grid representation, is not unitary, we therefore use a simple method to retain the unitarity of the propagator. Specifically, we renormalize the wave function after it has been propagated by the operator $e^{-iV\Delta}$. The detailed procedure has been described in refs 27 and 29.

C. Potential-Averaged Treatment for Rigid Bonds. For a polyatomic reaction with a nonreactive bond, such as the OH bond in the H_2 + OH reaction, one often does not have to treat the nonreactive OH bond length explicitly in the dynamics calculation. The PA5D model treats the vibration of the nonreactive CD bond diabatically which results in an effective 5D model in which the effective 5D potential is simply obtained by averaging the original PES over the vibrational function of the nonreactive CD (or OH) bond. Specifically, the interaction potential $V(\vec{r}_1, \vec{r}_2, \vec{R})$ in eq 2.9 is obtained by averaging the 6D potential over the vibrational function of the nonreactive CD,[23] *i.e.*,

$$V(\vec{r}_1, \vec{r}_2, \vec{R}) = \langle\phi_{v_2}|V(\vec{r}_1, \vec{r}_2, \vec{R})|\phi_{v_2}\rangle \qquad (2.14)$$

and the rotation constant for the nonreactive diatom CD is given by $B_{v_2} = \left\langle\phi_{v_2}\middle|1/2\mu_2 r_2^2\middle|\phi_{v_2}\right\rangle$. The study in ref 23 showed that the PA5D treatment is significantly better than the simpler rigid-bond treatment and that it gives reaction probabilities that are essentially indistinguishable from those of full 6D calculation for the OH + H_2 reaction. This is very encouraging for polyatomic reactions because it demonstrates the practicality of eliminating the spectator bond lengths from explicit dynamics calculations.

D. Extraction of Initial State-Selected Dynamics. From the propagation of an initial wavepacket $|\chi_i(0)\rangle$, the time-independent (TI) wave function $\psi_i^{+}(E)$ can be obtained by Fourier transforming the TD wave function[23]

$$\psi_i^{+}(E) = \frac{1}{2\pi a_i(E)}\int_{-\infty}^{\infty} e^{i/\hbar(E-H)t}\chi_i(0)\,{\rm d}t \qquad (2.15)$$

and similarly for the derivative of the wave function $\psi_i^{+'}(E)$. The coefficient $a_i(E)$ is easily evaluated from the free-energy-normalized asymptotic function $\phi_i(E)$ as $a_i(E) = \langle\phi_i(E)|\chi_i(0)\rangle$.[23] The total reaction probability from a given initial state i can be calculated by using the flux formula[23]

$$P_i^R(E) = \sum_f |S_{fi}^R|^2 = \langle\psi_i^{+}(E)|\hat{F}|\psi_i^{+}(E)\rangle \qquad (2.16)$$

The initial wavepacket $|\chi_i(0)\rangle$ is usually chosen to be a Gaussian function with an average momentum $k_{\rm O}$ traveling toward the interaction region

$$\phi_{k_{\rm O}}(R) = \left(\frac{1}{\pi\delta^2}\right)^{1/4}\exp[-(R-R_0)^2/2\delta^2]e^{-ik_0R} \qquad (2.17)$$

multiplied by the internal function $|\eta_i\rangle$ in eq 2.3. In actual propagation, the TD wavefunction is absorbed at the edges of the grid to avoid boundary reflection.[44]

E. Extraction of State-to-State Dynamics. The simplest approach to extract state-to-state **S** matrix elements or reaction probabilities is to explicitly write down the asymptotic form of the time-independent solution in the product arrangement space

$$\psi_{\alpha i}^{+}(E) \xrightarrow{R_\beta\to\infty} \sqrt{\frac{\mu_\beta}{2\pi\hbar^2}}\left[-\frac{e^{-ik_i R_\alpha}}{\sqrt{k_i}}\Big|\eta_{\alpha i}\rangle\delta_{\alpha\beta} + \sum_m S_{\beta m,\alpha i}\frac{e^{ik^m R_\beta}}{\sqrt{k_m}}\Big|\eta_{\beta m}\rangle\right] \qquad (2.18)$$

where the first term in the above equation vanishes for $\beta \neq \alpha$. Using eqs 2.15 and 2.18, it is straightforward to obtain the following expression for the state-to-state **S** matrix element

$$S_{fi}(E) = \frac{1}{a_{\alpha i}(E)}\sqrt{\frac{k_f}{2\pi\mu_\beta}}\,e^{-ik_f R_\infty}\int_{-\infty}^{\infty}{\rm d}t\,e^{i/\hbar Et}\langle R_\infty|\langle\eta_{\beta f}|\chi_{\alpha i}(t)\rangle$$

$$= \frac{1}{a_{\alpha i}(E)}\sqrt{\frac{k_f}{2\pi\mu_\beta}}\,e^{-ik_f R_\infty}\int_{-\infty}^{\infty}{\rm d}t\,e^{i/\hbar Et}A_{fi}(R_\infty, t) \qquad (2.19)$$

In the above approach, one simply calculates the amplitude of the scattering wave function A_{fi} (after projecting out the final states) by Fourier transforming the TD wavefunction at a dividing surface in the product asymptotic region. However, the asymptotic radial function has to be known exactly at the dividing surface, being plane wave function or Hankel function (see discussion in ref 45). For example, if at R_∞, the radial asymptotic solution is the function $B_f(R_\infty)$ instead of the plane wave, one needs to replace $e^{-ik_f R_\infty}(R_\infty)$ in eq 2.19.

If one only wants the absolute value of the **S** matrix element $|S_{fi}|$ or the probability $P_{fi} = |S_{fi}|^2$, e.g., for calculations of integral cross sections, one can use the flux formalism to calculate reaction probabilities,

$$|S_{fi}|^2 = 2\pi\hbar Re\,[A_{fi}^{*}(R_\beta, E)\hat{v}_\beta A_{fi}(R_\beta, E)]|_{R_\beta=R_L}$$

$$= \frac{2\pi\hbar^2}{\mu_\beta}\,Im\left[A_{fi}^{*}(R_\beta, E)\,\frac{d}{dR_\beta}A_{fi}(R_\beta, E)\right]|_{R_\beta=R_L} \qquad (2.20)$$

where $A_{fi}(E, R_\beta)$ is the radial scattering amplitude obtained from

$$A_{fi}(R_\beta, E) = \langle R_\beta|\langle\nu_{\beta f}|\psi_{\alpha i}^{+}(E)\rangle$$

$$= \frac{1}{2\pi\hbar a_{\alpha i}(E)}\int_{-\infty}^{\infty}{\rm d}t\,{\rm e}^{i/\hbar Et}\langle R_\beta|\langle\eta_{\beta f}|\chi_{\alpha i}(t)\rangle$$

$$= \frac{1}{2\pi\hbar a_{\alpha i}(E)}\int_{-\infty}^{\infty}{\rm d}t\,e^{i\hbar Et}A_{fi}(R_\beta, t) \qquad (2.21)$$

The flux is calculated at a surface defined by $R_\beta = R_L$ in the product asymptotic space beyond which the final state interaction is over. Therefore the flux is invariant with respect to further increase of the distance. The main advantage of using this flux formula is that one does not need to know the exact form of the radial function at R_L. Physically speaking, this is because the elastic scattering only affects the phase of the radial function and thus does not affect transition probabilities. This will in general enable one to obtain converged state-to-state reaction probability at a relatively shorter radial distance.

III. Applications to Four-Atom Reactions

A. Initial State-Selected Study for the H_2 + OH Reaction. In this subsection, we show some results of application of the

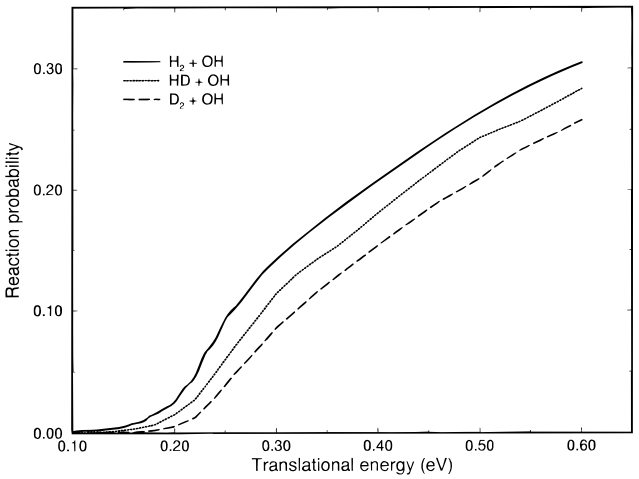

Figure 2. Comparison of reaction probability for all three reactions from initial ground state of the reactant.

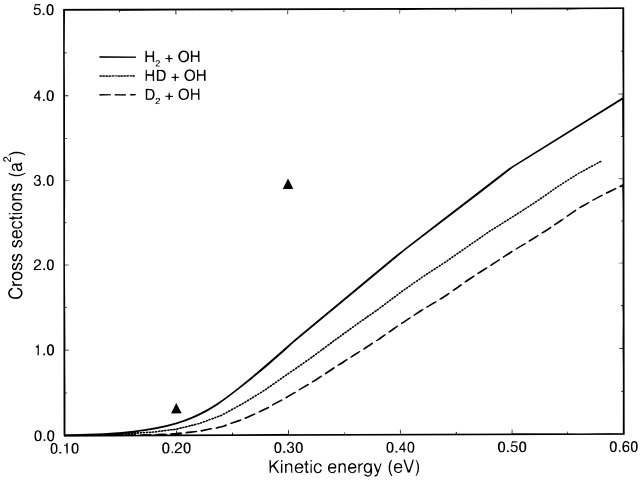

Figure 3. Comparison of integral cross sections for all three reactions from initial ground state of the reactant. The triangles are the RBA (rotating bond approximation) cross sections from ref 47 for H_2 + OH.

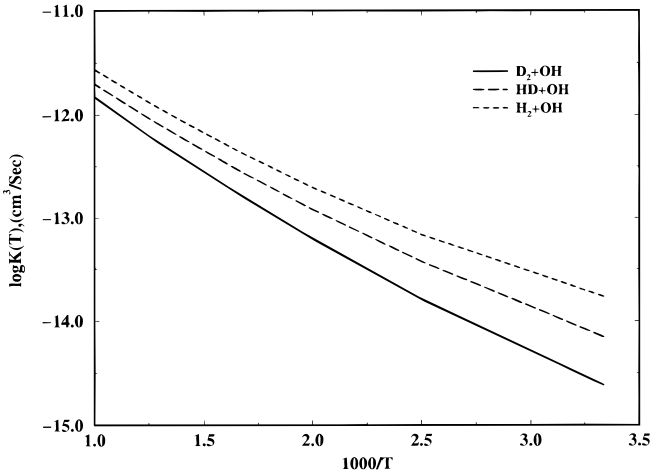

Figure 4. Comparison of reaction rate constants for all three reactions from initial ground state of the reactant.

TD approach described in the previous section for calculations of total (final state summed) reaction probabilities and cross sections for H_2 + OH and its isotopically substituted reactions HD + OH and D_2 + OH. The details of the calculation are not given here since they have been reported previously. The potential energy surface (PES) used for H_2 + OH reaction is the Walch−Dunning−Schatz−Elgersma PES[46] slightly modified by Clary.[47]

The calculation for H_2 + OH reaction in ref 23 demonstrated that the potential averaged treatment (PA5D) gives essentially the same result as the full 6D treatment for this reaction. Thus, the potential averaged treatment for the nonreactive bond is sufficiently accurate at least for total reaction probabilities, and the 6D reactive scattering problem can be effectively reduced to a 5D problem. We expect this conclusion to be generally true for similar reactions involving nonreactive or spectator bonds. This should result in significant savings in computational effort for polyatomic reactions.

In Figure 2, we show reaction probabilities of all three isotopic reactions as a function of incident kinetic energy from the initial ground state. The reaction probability is of the order $P(H_2) > P(HD) > P(D_2)$ at fixed kinetic energies. However, considering the vibrational energy difference among H_2, HD, and D_2, the reaction probability is about the same magnitude as a function of total energy (kinetic energy + zero-point energy). The study on the rotational state dependence of the reaction probability shows strong steric effect as discussed in refs 26−28. In particular, the maximum of the reaction probability always shows up for the $j = 1$ state of $H(D)_2$, which is believed to be a general phenomenon for collinearly dominated reactions at zero total angular momentum.[26] In addition, the vibrational excitation of H_2 is found to significantly enhance the reaction probability while vibrational excitation of the nonreactive OH(D) bond has little effect on reaction.[23]

The reaction cross section for a specific initial state is obtained by summing the reaction probabilities $P^{J\epsilon}_{v_0 j_0 K_0}$ over all the partial waves (total angular momentum J),

$$\sigma_{v_0 j_0}(E) = \frac{1}{(2j_1+1)(2j_2+1)} \frac{\pi}{k^2} \sum_{JK_0\epsilon} (2J+1) P^{J\epsilon}_{v_0 j_0 K_0}(E) \tag{3.1}$$

where ϵ is the parity and K_O denotes all the initial rotation projection quantum numbers. Since the exact close-coupling calculation for $J > 0$ is extremely expensive computationally, the standard CS approximation[48,49] is used in calculations for $J > 0$. For the H_2 + OH reaction at ground initial state, the cross sections for all three reactions as a function of kinetic energy are shown in Figure 3. The order of cross sections, as a function of kinetic energy, satisfies $\sigma_{H_2} > \sigma_{HD} > \sigma_{D_2}$. We also show the cross sections from the reduced dimensionality calculation (RBA) of ref 47. The comparison shows that the RBA cross sections are significantly larger than the full-dimensional results.

The initial state-specific thermal rate constant is given in terms of the total integral cross section of eq 3.1 by

$$r_{v_0 j_0}(T) = \left(\frac{1}{2}\right)\left(\frac{8kT}{\pi\mu}\right)^{1/2} (kT)^{-2} \int_0^\infty dE_t E_t \exp(-E_t/kT) \sigma_{v_0 j_0}(E_t) \tag{3.2}$$

where E_t is the translational energy. An extra factor of $^1/_2$ has been included in eq 3.2 to account for the fact that only half of the reagent $H_2(^1\Sigma)$ + $OH(^2\pi)$ collisions access the $^2A'$ surface which correlates with the products $H_2O(^1A')$ + $H(^2A')$.[46] We note that the thermal rate constant defined in the above equation involves only Boltzmann averaging over translational energy but not rotational energy. This is not the standard definition of thermal rate constant in which all the rotational states are Boltzmann averaged. Therefore, comparisons of the present rate constants with experimental and other theoretical calculations should be treated with caution. At temperatures below 1000 K, the rate constant for the H_2 + OH and its isotope

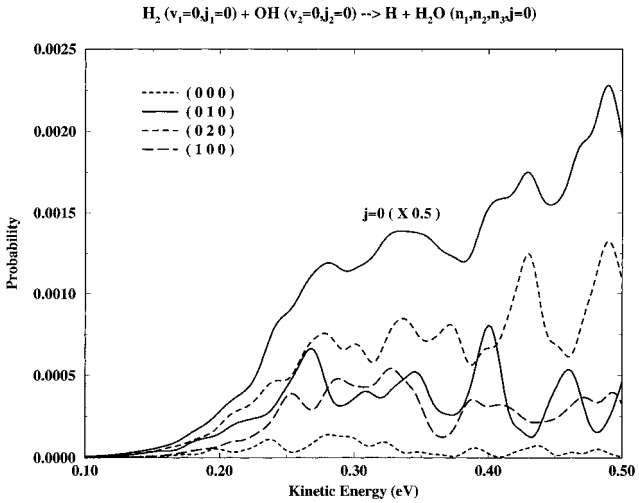

Figure 5. Energy dependence of product vibrational state-specific reaction probabilities from the reaction OH(00) + H_2(00) → H_2O (v,j = 0) for zero total angular momentum of H_2OH. The vibrational state label of H_2O (ν_1, ν_2, ν_3) follows the standard definition for triatomic systems. Only the first four open vibrational states are explicitly shown. The vibration-summed reaction probability (the upper most curve) was scaled by a factor of 0.5 before being plotted.

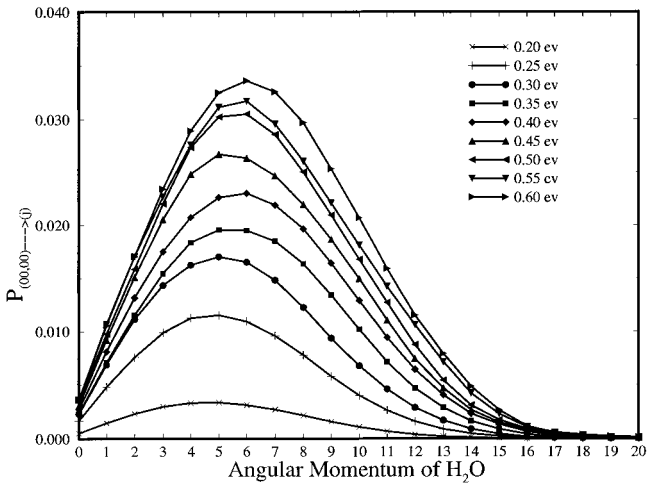

Figure 6. Product rotational state distribution of H_2O from the reaction H_2(00) + OH(00) → H + H_2O(j) summed over all vibrational states for kinetic energies of 0.10−0.6 eV.

reactions satisfies the relation $k_{H_2} > k_{HD} > k_{D_2}$. These relationships are somehow similar to the triatomic reaction of O + H_2 and its isotope reactions.[50−53] In view of the deficiencies of the WDSE potential energy surface and the fact that theoretical rates are not thermally averaged over the initial states, the agreement of theoretical rate constant with experimental measurement is quite reasonable as discussed in ref 23.

Our study also found that the WDSE PES has artifacts that cause artificial resonances at very low kinetic energies (about 0.02 eV).[23] The artifacts have a significant effect on the calculated integral cross sections and rate constants for vibrationally excited H_2 for the reaction of H_2 + OH. The effect is less significant for vibrationally excited D_2 in D_2 + OH reaction and is negligible for reactions involving ground vibration of H_2 + OH.

B. State-to-State Study for H_2 + OH → H + OH_2. Ultimately one wants to calculate state-to-state dynamical quantities such as state-to-state integral cross sections and/or differential cross sections for tetraatomic reactions. The state-to-state calculation is significantly more difficult computationally than the calculation of total (final state summed) reaction probabilities. For H_2 + OH → H + H_2O, the reaction probabilities are calculated by using the reactant Jacobi coordinates to propagate the wave-function all the way into the asymptotic space of the product arrangements.[30,31] Figure 5 shows the energy-dependence of reaction probabilities from the ground state of H_2 + OH to produce various rovibrational states of H_2O.[31] These individual probabilities show oscillatory structures as a function of kinetic energy. The reaction seems to produce more bending excited H_2O as shown in Figure 5 where (020) and (010) products of H_2O have relatively larger reaction probabilities than (000) and (100) states. In particular, the population of the ground vibrational state of H_2O is very small. By the principle of microreversibility, this implies that the probability of the reverse reaction H + H_2O is very small if the water reactant is in the ground vibrational state.

Figure 6 shows a complete rotational state distribution of H_2O (summed over vibrational states of H_2O) at kinetic energies between 0.2 and 0.6 eV.[30] These distributions are Boltzmann-like with the rotation quantum number of corresponding to the maximum distribution increases from around $j = 4-6$ as the collision energy increases.

Recently, state-to-state calculation has also been reported by Zhang and Light for the reverse reaction H + H_2O → H_2 + OH.[33] All these state-to-state calculations, however, used a single set of Jacobi coordinates for the reactant arrangement to propagate the wave function all the way into the product asymptotic space. Therefore the current method is computationally expensive for state-to-state dynamics calculations because one has to employ a larger basis set and numerical grid in order to cover physically relevant spaces for both reactant and product arrangements.

At this stage, the progress in theoretical quantum dynamics studies for H_2 + OH reaction is challenging both the experimentalists and quantum chemists. Firstly, accurate new PES needs to be calculated using high level *ab initio* methods in order to match the accuracy of the dynamics calculation for H_2 + OH reaction. Secondly, we need state-to-state experimental results for detailed comparison of the dynamics for this reaction.

C. HO + CO Reaction. The quantum dynamics calculation for HO + CO reaction is much more challenging computationally than the direct H_2 + OH reaction. First, the mass of HOCO system is heavier, and secondly, the HO + CO reaction is dominated by resonances due to the existence of deep wells supporting stable species of *cis*- and *trans*-HOCO complexes.[54] Previous quantum dynamics calculations were carried out in 2D,[55] 3D,[20,56,57] and 4D (planar).[20] The dynamics calculation reported in ref 29 is the first quantum calculation in full physical space using the PA5D treatment in which the nonreactive CO bond is treated diabatically. The TD calculation for HO + CO requires one to propagate the wavefunction to more than 1 ps in order to reveal resonance structures.[29]

We show in Figure 7 the total reaction probability from three different rotational states of the reagents as a function of kinetic energy for zero total angular momentum ($J = 0$). There are many narrow resonances that overlap with neighboring ones as can be seen in Figure 7. Although the reaction is exothermic by about 0.97 eV and there is no barrier in the entrance channel, the reaction probability is generally small (less than 10% in Figure 7). The system does not seem to follow the reaction path and therefore produces very little reaction, although the HO + CO PES has only a negligible entrance barrier along the minimum energy path. From the propagation time needed to converge the reaction probabilities, the lifetimes of most

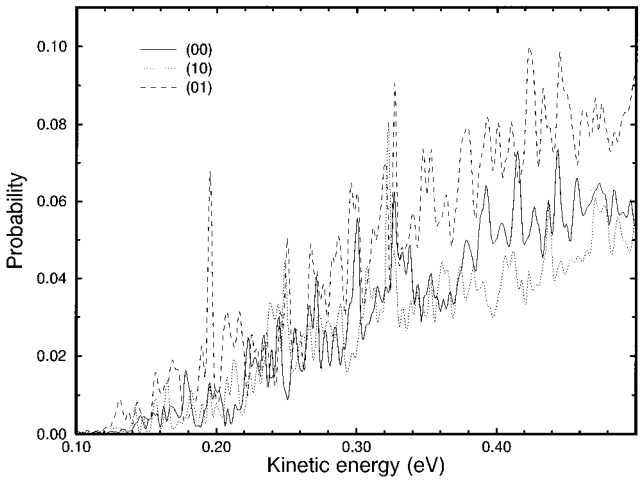

Figure 7. Reaction probabilities of HO($v = 0,j_1$) + CO($v = 0,j_2$) as functions of kinetic energy for (j_1j_2)=(00), (10), and (01).

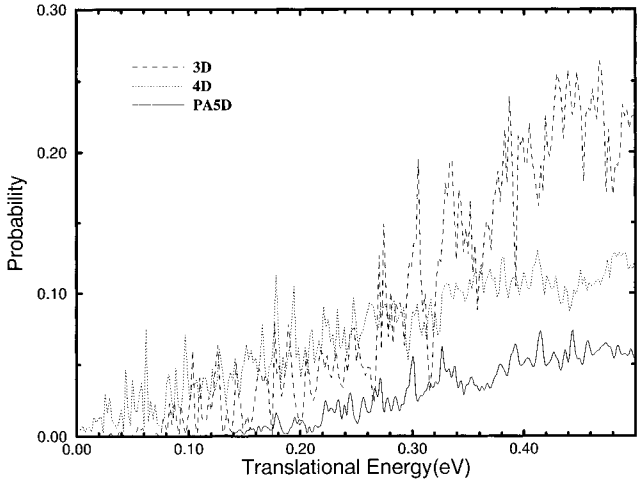

Figure 8. Comparison of present result with reduced dimensionality calculations from ref 20. Dashed curve and dotted curve are 3D and 4D results from ref 20, respectively. Solid curve is the PA5D result from the present calculation.

resonances are less than 1 ps with only a couple of them lasting a little longer than that.

Although there are many similarities between the results of the present calculation and previous reduced dimensionality calculations, the present reaction probabilities are considerably smaller in magnitude than those of reduced dimensionality calculations in 3D and 4D[20] as shown in Figure 8, underscoring the importance of the multidimensional nature of the dynamics. There are two possible reasons for the results of reduced dimensionality calculations to be too large. First, the reduced dimensionality calculations did not take into proper account the zero-point energies associated with the neglected degrees of freedom. Second, the reduced dimensionality calculations only sampled most favorable geometry for reaction. It is thus interesting to note that an earlier reduced dimensionality calculation of Clary and Schatz[56] gave the magnitude of reaction probabilities in better agreement with the present results. Obviously, there are uncertainties in how to properly take into account the effect of neglected degrees of freedom in various reduced dimensionality calculations.

IV. A New Approach to State-to-State Reactive Scattering

A. A General Reactant−Product Decoupling Scheme. The procedure to extract state-to-state dynamics information, after the TD wave function has been propagated all the way into the asymptotic product space, is straightforward as shown in the previous section. The most difficult part is the determination of the wave function that is correct in the product asymptotic space. We therefore encounter the notorious problem of the choice of coordinates in quantum reactive scattering again. If only total reaction probability is needed, one can more or less avoid this problem by using the reactant Jacobi coordinates as described previously. Although for state-to-state calculations one could still use a single set of Jacobi coordinates (either reactant or product) to carry out the wavefunction propagation throughout the whole space, it can only be done at an immense computational cost as demonstrated in recent state-to-state calculations for the $H_2 + OH$ reaction.[30,31,33] We recently developed a general reactant−product decoupling (RPD) scheme using the idea of divide and conquer to treat state-to-state reactive scattering problems.[58] In this approach, one partitions the full wavefunction into the reactant and a sum of all product components:

$$\Psi(t) = \Psi_r(t) + \sum_p \Psi_p(t) \tag{4.1}$$

where r and p are labels of reactant and product arrangements, respectively. Since we only require the full wavefunction $\Psi(t)$ to satisfy the TD Schrödinger equation, there is considerable freedom in choosing the individual component. Our main criterion is to confine each component to its corresponding arrangement space with a minimum amount of overlap with other components. For this purpose, we devise the following *uncoupled* equations,

$$\begin{cases} i\hbar\dfrac{\partial}{t}|\Psi_r(t)\rangle = H|\Psi_r(t)\rangle - i\sum_p V_p|\Psi_r(t)\rangle \\ i\hbar\dfrac{\partial}{\partial t}\Psi_p(t)\rangle = H|\Psi_p(t)\rangle + iV_p|\Psi_r(t)\rangle \end{cases} \tag{4.2}$$

where $-iV_p$ is the negative imaginary potential (absorbing potential) placed just beyond the transition state region to block the wave function $\Psi_r(t)$ from entering the p product arrangement space. The $\Psi_r(t)$ in eq 4.2 can be calculated using the reactant Jacobi coordinates, exactly as discussed in previous sections for the calculation of total reaction probabilities. The only extra effort required here is to write out the quantity $V_p\Psi_r(t)$ on the strips of absorbing potential for the desired product arrangement(s) to a computer disk for later use.

Assuming the wave function $\Psi_r(t)$ is perfectly absorbed without any reflection, the $\Psi_r(t)$ is then the correct representation of the full wave function in spaces before the turning on of absorbing potentials. Thus the product wavefunction $\Psi_p(t)$ needs to be nonzero only in the corresponding pth product space starting from where V_p is turned on. The solution of $\Psi_p(t)$ is therefore an inelastic scattering one and its propagation can be naturally carried out using the product Jacobi coordinates, independent of the rest of the product arrangements A split-operator propagator can be found for $\Psi_p(t)$[58]

$$|\tilde{\Psi}_p(t+\Delta)\rangle = e^{-i/\hbar H\Delta}|\tilde{\Psi}_p(t) + \frac{\Delta}{\hbar}V_p|\Psi_r(t+\Delta)\rangle \tag{4.3}$$

where $\tilde{\Psi}_p(t) = \Psi_p(t) + \Delta / 2\hbar V_p|\Psi_r(t)$.

The calculations for $\Psi_r(t)$ and $\Psi_p(t)$ are relatively straightforward by using their respective Jacobi coordinates. The main tricky part of this scheme is to make sure that the absorbing potentials are smooth enough to prevent any wavefunction reflection and to generate $V_p\Psi_r(t)$ in the product arrangement basis representation in eq 4.3. The former has to be checked

by numerical convergence test in actual calculations, and the latter requires a coordinate transformation between the Jacobi coordinates of the reactant and product arrangements. Since the coordinate transformation for $V_p\Psi_r(t)$ has to be done at each time step, it is crucial to use highly efficient quadrature schemes to minimize the number of points in generating $V_p\Psi_r(t)$. We show in the following a highly efficient quadrature scheme based on the general theory of collocation method for our particular application.

B. A Multidimensional Collocation-Quadrature Scheme. Our motivation is to devise an efficient quadrature method with the least number of quadrature points to accurately evaluate the following integral

$$I_n = \langle n|f\rangle \tag{4.4}$$

by a finite summation

$$I_n \approx \sum_i W_{ni} f_i \tag{4.5}$$

where $n(q)$ are N linearly independent basis functions, q_i are N pre-fixed quadrature points, $f_i = f(q_i)$, and $\mathbf{W}$ is an undetermined weighting matrix. For simplicity, we deal with a one-dimensional model and orthogonal basis set although the method can be trivially generalized to multidimensional case and to nonorthogonal and nondirect product basis set. If we assume that the function f can be adequately represented by an expansion in terms of N basis functions $n(q)$, we then require that eq 4.5 be exact! Thus we obtain the matrix equation

$$\mathbf{WN} = \mathbf{I} \tag{4.6}$$

where $N_{in} = n(q_i)$ and $\mathbf{I}$ is the identity matrix. The solution to eq 4.6 determines the matrix $\mathbf{W}$

$$\mathbf{W} = \mathbf{N}^{-1} \tag{4.7}$$

Thus for any function f the integral in eq 4.4 can be numerically evaluated as

$$I_n = [N]^{-1}_{ni} f_i \tag{4.8}$$

and the error of the integral is directly related to the incomplete representation of the function f by the N basis functions $n(q)$. Equation 4.8 can also be viewed as a general transformation relation between basis representation I_n and pointwise representation f_i of the function $f(q)$, except that the transformation matrix is in general not unitary here. This quadrature scheme for evaluating the integral in eq 4.4 is actually a special application of a general theory called collocation method.[59]

The above quadrature scheme is quite general and can be applied when basis functions are nonorthogonal, multidimensional, and nondirect product. We can now generalize eq 4.7 to

$$\mathbf{W} = \mathbf{N}^{-1}\mathbf{O} \tag{4.9}$$

where $O_{mn} = \langle m|n\rangle$ is the overlap matrix of the basis functions and the quadrature points are now multidimensional and denoted as $\bar{q}_i$. So far the choice of quadrature points $\bar{q}_i$ has not been discussed and in principle they can be arbitrary chosen as long as the inverse in eq 4.7 exists. However, a good choice will help reduce the error due to the incompleteness of the basis set. For one-dimensional basis functions, a natural choice of points would be those obtained from discrete variable representation (DVR) method.[60,61] The systematic choice of quadrature points for multidimensional, nondirect product basis functions is not obvious at all and needs to be explored in the future.

Excellent state-to-state results have recently been obtained for the atom−diatom reactions H + H_2[62] and D + H_2.[63] At this stage, it is very promising to extend the RPD approach to tetraatomic reactions and beyond.

V. Discussions and Conclusions

We have provided a current account of the recent development in TD quantum wavepacket approach to tetraatomic reaction dynamics including the most recent RPD (reactant-product decoupling) method for state-to-state reactive scattering dynamics. Various numerical techniques for practical applications are also presented in considerable detail. Specific applications of the TD methods and the results of those applications to several tetraatomic reaction systems are shown as demonstrations, with special emphasis given to the benchmark H_2 + OH reaction including the most recent state-to-state results. In particular, we would like to reiterate the general nature of the RPD method presented in this paper and its important applications as a highly efficient computational approach for studying state-to-state reaction dynamics for polyatomic systems using the strategy of divide and conquer. The collocation-quadrature (CQ) scheme presented in this article is a general and efficient numerical approach for fast and accurate evaluation of integrals involving a basis set expansion. Its potential application to integrals involving multidimensional, nondirect product basis functions is very promising. Test applications of the RPD method, combined with the collocation-quadrature (CQ) scheme, to the three-dimensional state-to-state calculation for H + H_2[62] and D + H_2[63] show excellent results. Further extensions of the RPD method to more general applications are also being reported.[64]

We believe that the TD approach currently provides the best hope for further extending accurate quantum dynamics studies to polyatomic reaction systems involving more than four atoms due to its relatively slow scaling of computational effort with the number of basis functions (cpu $\propto N^{\alpha}$ $(1 < \alpha < 2)$). For this purpose, we need to further develop efficient numerical techniques to make dynamics calculations possible for even larger systems. There are several aspects for future development of TD methods for applications to larger polyatomic systems. First, one should always try to minimize the total number of active degrees of freedom for a given polyatomic system by identifying those nonreactive or spectator coordinates and treating them either adiabatically or diabatically without much loss of dynamics information, and thereby eliminating them from explicitly coupled dynamics calculations. Second, we need to develop more efficient basis function optimization techniques in order to drastically reduce the number of basis functions in the wave function expansion.

Finally, in view of the recent rapid progress in the development of accurate quantum dynamics methods for reaction dynamics, it is very important to call for developing more accurate and reliable means for fast calculation of potential energy surfaces for chemical reaction systems if we want to study reaction dynamics correctly, make closer contact with experiments, and make reliable dynamical predictions. The recent development of dynamical theory is also challenging the experiment to produce reliable state-to-state dynamical quantities for detailed comparison with theoretical predictions.

Acknowledgment. We thank Dr. Dong H. Zhang who has done much of the calculations presented in this article and has

helped us very much during the course of our work. We also thank Dunyou Wang for some of the calculations presented in this article. We acknowledge financial support from the Division of Chemical Sciences, Office of Basic Energy Sciences, U.S. Department of Energy, under Grant DE-FG02-94ER114453; National Science Foundation through a presidential Faculty Fellows Award; the Donors of Petroleum Research Fund; the A.P. Sloan Foundation, and the Camille and Henry Dreyfus Foundation.

References and Notes

(1) Schatz, G. C.; Kuppermann, A. *J. Chem. Phys.* **1976**, *65*, 4642.
(2) Miller, W. H. *Annu. Rev. Phys. Chem.* **1990**, *41*, 245 and references therein.
(3) (a) Haug, K.; Schwenke, D. W.; Shima, Y.; Truhlar, D. G.; Zhang, J. Z. H.; Kouri, D. J. *J. Phys. Chem.* **1986**, *90*, 6757. (b) Zhang, J. Z. H.; Kouri, D. J.; Haug, K.; Schwenke, D. W.; Shima, Y.; Truhlar, D. G. *J. Chem. Phys.* **1988**, *88*, 2492. (c) Schwenke, D. W.; Haug, K.; Zhao, M.; Truhlar, D. G.; Sun, Y.; Zhang, J. Z. H.; Kouri, D. J. *J. Phys. Chem.* **1988**, *92*, 3202. (d) Mladenovic, M.; Zhao, M.; Truhlar, D. G.; Schwenke, D. W.; Sun, Y.; Kouri, D. J. *J. Phys. Chem.* **1988**, *92*, 7035.
(4) (a) Zhang, J. Z. H.; Miller, W. H. *Chem. Phys. Lett.* **1988**, *153*, 465. (b) Zhang, J. Z. H.; Chu, S-I; Miller, W. H. *J. Chem. Phys.* **1988**, *88*, 6233. (c) Zhang, J. Z. H.; Miller, W. H. *J. Chem. Phys.* **1989**, *91*, 1528. (d) *Ibid.* **1990**, *92*, 1811. (e) *Ibid.* **1990**, *94*, 7785.
(5) (a) Manolopoulos, D. E.; Wyatt, R. E. *Chem. Phys. Lett.* **1988**, *152*, 23. (b) *Ibid. J. Chem. Phys.* **1989**, *91*, 6096. (c) Manolopoulos, D. E.; D'Mello, M.; Wyatt, R. E. *J. Chem. Phys.* **1990**, *93*, 403.
(6) (a) Parker, G. A.; Pack, R. T.; Archer, B. J.; Walker, R. B. *Chem. Phys. Lett.* **1987**, *137*, 564. (b) Pack, R. T.; Parker, G. A. *J. Chem. Phys.* **1987**, *87*, 3888. (c) Kress, J. D.; Bacic, Z.; Parker, G. A.; Pack, R. T. *Chem. Phys. Lett.* **1989**, *157*, 484.
(7) (a) Kuppermann, A.; Hipes, P. G. *J. Chem. Phys.* **1986**, *84*, 5962. (a) A. Kuppermann, *Advances in Molecular Vibrations and collision Dynamics*; Bowman, J., Ed.; JAI Press: Greenwich, CT, 1994; Vol. 2B, p 117.
(8) Schatz, G. C. *Chem. Phys. Lett.* **1988**, *150*, 92.
(9) Linderberg, J. *Int. J. Quantum Chem., Quantum Chem. Symp.* **1986**, *19*, 467.
(10) (a) Launay, J. M.; Dourneuf, M. L. *Chem. Phys. Lett.* **1989**, *163*, 178. (b) *Ibid.* **1990**, *169*, 473.
(11) (a) Zhang, J. Z. H. *J. Chem. Phys.* **1991**, *94*, 6047. (b) *Ibid. Chem. Phys. Lett.* **1991**, *181*, 63.
(12) (a) Wu, Y. S. M.; Kuppermann, A.; Lepetit, B. *Chem. Phys. Lett.* **1991**, *186*, 319. (b) *Ibid.* **1993**, *201*, 178.
(13) Castillo, J. F.; Manolopoulos, D.; Stark, K.; Werner, H-J *J. Chem. Phys.* **1996**, *104*, 6531.
(14) (a) Sun, Q.; Bowman, J. M. *J. Chem. Phys.* **1990**, *92*, 5201; (b) Sun, Q.; Yan, D. L.; Wang, N. S.; Bowman, J. M.; Lin, M. C *J. Chem. Phys.* **1990**, *93*, 4730. (d) Bowman, J. M.; Wang, D. *J. Chem. Phys.* **1992**, *96*, 7852. (e) Wang, D.; Bowman, J. M. *J. Chem. Phys.* **1992**, *96*, 8906. (f) *Ibid.* **1993**, *98*, 6235. (g) *Ibid. Chem. Phys. Lett.* **1993**, *207*, 227.
(15) (a) Brook, A. N.; Clary, D. C. *J. Chem. Phys.* **1990**, *92*, 4178. (b) Clary, D. C. *J. Chem. Phys.* **1991**, *95*, 7298. (c) *Ibid.* **1992**, *96*, 3656. (d) Clary, D. C. *Chem. Phys. Lett.* **1992**, *192*, 34. (e) Nyman, G.; Clary, D. C. *J. Chem. Phys.* **1993**, *99*, 7774.
(16) (a) Szichman, H.; Last, I.; Baram, A.; Baer, M. *J. Phys. Chem.* **1993**, *97*, 6436. (b) Szichman, H.; Baer, M. *J. Chem. Phys.* **1994**, *208*, 101. *Chem. Phys. Lett.* **1995**, *285*, 242.
(17) Balakrishnan, N.; Billing, G. D. *J. Chem. Phys.* **1994**, *10*, 2785. *Iden. Chem. Phys.* **194**, *499*, 189.
(18) Echave, J.; Clary, D. C. *J. Chem. Phys.* **1994**, *100*, 402.
(19) Thompson, W. H.; Miller, W. H. *J. Chem. Phys.* **1994**, *101*, 8620.
(20) Goldfield, E. M.; Gray, S. K.; Schatz, G. C. *J. Chem. Phys.* **1995**, *102*, 8807.
(21) Zhang, D. H.; Zhang, J. Z. H. *J. Chem. Phys.* **1993**, *99*, 5615.
(22) Zhang, D. H.; Zhang, J. Z. H. *J. Chem. Phys.* **1994**, *100*, 2697.
(23) Zhang, D. H.; Zhang, J. Z. H. *J. Chem. Phys.* **1994**, *101*, 1146.
(24) (a) Manthe, U.; Seideman, T.; Miller, W. H. *J. Chem. Phys.* **1993**, *99*, 10078. (b) Manthe, U.; Seideman, T.; Miller, W. H. *J. Chem. Phys.* **1994**, *101*, 4759.
(25) Neuhauser, D. *J. Chem. Phys.* **1994**, *100*, 9272.
(26) Zhang, D. H.; Zhang, J. Z. H. *Chem. Phys. Lett.* **1995**, *232*, 370.
(27) Zhang, D. H.; Zhang, J. Z. H.; Zhang, Y.; Wang, D.; Zhang, Q. *J. Chem. Phys.* **1995**, *102*, 7400.
(28) Zhang, Y.; Zhang, D.; Li, W. Zhang; Q., Wang, D.; Zhang, D. H.; Zhang, J. Z. H. *J. Phys. Chem.* **1995**, *99*, 16824.
(29) Zhang, D. H.; Zhang, J. Z. H. *J. Chem. Phys.* **1995**, *103*, 6512.
(30) Zhu, W.; Dai, J.; Zhang, J. Z. H. *J. Chem. Phys.* **1996**, *105*, 4881.
(31) Dai, J.; Zhu, W.; Zhang, J. Z. H. *J. Phys. Chem.* **1996**, *100*, 13901.
(32) Zhang, D. H.; Light, J. C. *J. Chem. Phys.* **1996**, *104*, 4544.
(33) Zhang, D. H.; Light, J. C. *J. Chem. Phys.* **1996**, *105*, 1291.
(34) Zhang, D. H.; Zhang, J. Z. H. In *Dynamics of Molecules and Chemical Reactions*; Wyatt, R. E., Zhang, J. Z. H., Ed.; Marcel Dekker: New York, 1996, p 231.
(35) Mowrey, R. C.; Kouri, D. J. *J. Chem. Phys.* **1986**, *84*, 6466.
(36) Kosloff, R. *J. Phys. Chem.* **1988**, *92*, 2087.
(37) Neuhauser, D.; Baer, M.; Judson, R. S.; Kouri, D. J. *Comput. Phys. Commun.* **1991**, *63*, 460.
(38) Mowrey, R. C. *J. Chem. Phys.* **1991**, *94*, 7098.
(39) Sharafeddin, O. A.; Zhang, J. Z. H. *Chem. Phys. Lett.* **1993**, *204*, 190.
(40) Zhang, D. H.; Zhang, J. Z. H. *J. Chem. Phys.* **1993**, *98*, 6276.
(41) Zhang, D. H.; Zhang, J. Z. H. *J. Chem. Phys.* **1993**, *99*, 6624.
(42) Rose, M. E. *Elementary Theory of Angular Momentum*; Wiley: New York, 1957.
(43) Fleck, J. A.; Morris, J. R., Jr.; Feit, M. D. *Appl. Phys. (Berlin)* **1976**, *10*, 129.
(44) (a) Neuhauser, D.; Baer, M. *J. Chem. Phys.* **1989**, *91*, 4651. (b) Neuhauser, D.; Baer, M.; Kouri, D. J. *J. Chem. Phys.* **1990**, *93*, 2499.
(45) Dai, J.; Zhang, J. Z. H. *J. Phys. Chem.* **1996**, *100*, 6898.
(46) (a) Walch, S. P.; Dunning, T. H., Jr. *J. Chem. Phys.* **1980**, *72*, 1303. (b) Schatz, G. C.; Elgersma, H. *Chem. Phys. Lett.* **1980**, *73*, 21.
(47) Clary, D. C. *J. Chem. Phys.* **1991**, *95*, 7298.
(48) McGuire, P.; Kouri, D. J. *J. Chem. Phys.* **1974**, *60*, 2488.
(49) Pack, R. T. *J. Chem. Phys.* **1974**, *60*, 633.
(50) Presser, N.; Gordon, R. J. *J. Chem. Phys.* **1985**, *82*, 1291.
(51) Garrett, B. C.; Truhlar, D. G.; Bowman, J. M.; Wagner, A. F.; Robie, D.; Arepalli, S.; Presser, N.; Gordon, R. J. *J. Am. Chem. Soc.* **1986**, *108*, 3515.
(52) Bowman, J. M.; Wagner, A. F. *J. Chem. Phys.* **1987**, *86*, 1967.
(53) Day, P. N.; Truhlar, D. G. *J. Chem. Phys.* **1991**, *95*, 5097.
(54) Schatz, G. C.; Fitzcharles; Harding, L. B. *Faraday Discuss.* **1987**, *84*, 359.
(55) Schatz, G. C.; Dyke, J. *Chem. Phys. Lett.* **1992**, *188*, 11.
(56) Clary, D. C.; Schatz, G. C. *J. Chem. Phys.* **1992**, *99*, 4578.
(57) Balakrishnan, N.; Billing, G. D. *J. Chem. Phys.* **1996**, *104*, 4004.
(58) Peng, T.; Zhang, J. Z. H. *J. Chem. Phys.* **1996**, *105*, 6072.
(59) Canuto, C.; Hussaini, M. Y.; Quarteroni, A.; Zhang, T. A. *Spectral Methods in Fluid Dynamics*; Springer: New York, 1988.
(60) Lill, J. V.; Parker, G. A.; Light, J. C. *Chem. Phys. Lett.* **1982**, *89*, 483.
(61) Bacic, Z.; Light, J. C. *Annu. Rev. Phys. Chem.* **1989**, *40*, 469.
(62) Zhu, W.; Peng, T.; Zhang, J. Z. H. *J. Chem. Phys.* In press.
(63) Dai, J.; Zhang, J. Z. H. *J. Chem. Soc., Faraday Trans.* In press.
(64) Kouri, D. J.; Hoffman, D. K.; Peng, T.; Zhang, J. Z. H. *Chem. Phys. Lett.* **262**, *519*, 1996.